# Course of explosion behaviour of metallic powders – From micron to nanosize

Alexis Vignes, Arne Krietsch, Olivier Dufaud, Audrey Santandrea, Laurent Perrin, Jacques Bouillard

▶ **To cite this version:**

Alexis Vignes, Arne Krietsch, Olivier Dufaud, Audrey Santandrea, Laurent Perrin, et al.. Course of explosion behaviour of metallic powders – From micron to nanosize. Journal of Hazardous Materials, 2019, 379, pp.120767. 10.1016/j.jhazmat.2019.120767 . hal-02372373

**HAL Id: hal-02372373**

**https://hal.univ-lorraine.fr/hal-02372373**

Submitted on 25 Oct 2021

**HAL** is a multi-disciplinary open access archive for the deposit and dissemination of scientific research documents, whether they are published or not. The documents may come from teaching and research institutions in France or abroad, or from public or private research centers.

L'archive ouverte pluridisciplinaire **HAL**, est destinée au dépôt et à la diffusion de documents scientifiques de niveau recherche, publiés ou non, émanant des établissements d'enseignement et de recherche français ou étrangers, des laboratoires publics ou privés.

Distributed under a Creative Commons Attribution - NonCommercial 4.0 International License

Version of Record: https://www.sciencedirect.com/science/article/pii/S0304389419307095
Manuscript_6a4050a58b80d50ff410d0aea2e091db

# Course of Explosion Behaviour of Metallic Powders – from Micron to Nanosize

Alexis Vignes[1], Arne Krietsch[2], Olivier Dufaud[3], Audrey Santandréa[1,3], Laurent Perrin[3], Jacques Bouillard[1]

[1] INERIS, Accidental Risks Division, Parc ALATA, BP 2, F-60550 Verneuil en Halatte, France

[2] BAM, Bundesanstalt für Materialforschung und -prüfung (BAM), Division 2.1 Explosion Protection Gases and Dusts, Unter den Eichen 87, 12205 Berlin

[3] Laboratoire Réactions et Génie des Procédés, Université de Lorraine, UMR 7274 CNRS-UL, 1 rue Granville, BP 20451, F-54001 Nancy, France

**Corresponding author:** Alexis Vignes (E-mail address: alexis.vignes@ineris.fr)

**Abstract:**

This work presents an overview about the explosion behaviour of metallic powders from micron to nanosize. Aluminium, magnesium, titanium, iron and zinc were considered and their explosion safety parameters were analysed as a function of their mean primary particle size either determined by BET measurements, particle size distribution. To depict the course of explosion behaviour for these metals, extensive literature review has been performed and additional experimental tests were also performed. Generally, decreasing the particle size in a metallic powder leads to a higher explosion severity. It appears that this statement is true till a critical diameter below which the explosion severity ($p_{max}$, $dp/dt_{max}$) decreases for all the considered powders. This critical size can be explained by theoretical considerations on the nature of thermal transfer in the flame, namely by analysing the Cassel model. Finally, semi-



© 2019 published by Elsevier. This manuscript is made available under the CC BY NC user license
https://creativecommons.org/licenses/by-nc/4.0/

empirical models were also developed for aluminium to highlight the specific micrometre and nanometre behaviour and the influence of turbulence, particle burning time, diameter and concentration. The influence of these key parameters needs to be further assessed in a future work in order to better understand the mechanisms involved and to extend the scope to other powdered materials.

**Keywords:** Dust Explosion, Metallic powders, Nanopowder, Nanomaterials

## 1. Introduction

Numerous studies have been carried out on assessing the explosivity of metallic dusts [1–3]. Only a minority of them concerns metallic nanopowders, probably due to the relative novelty of the use and production of such compounds. Most of the papers related to nanodust explosion are focused on reviewing the available data or providing data on ignition sensitivity and explosion severity of nanopowders [4–17]. Such data were produced so far either by standardised protocols [18,19] or through modified ones [20,21].

These studies as well as more fundamental work [22] on the flammability and explosivity of nanopowders are currently focusing on various aspects related to the specific properties of the nanopowders: their large surface area, their propensity for agglomeration, their high reactivity.

Pyrophoric behaviour of metal nanoparticles [23–26] was also investigated. Sundaram et al. [26] notably demonstrated that aluminium particles having oxide layers thicker than 0.3 nm can be considered as non-pyrophoric. Other authors worked on the assessment of the influence of passivation on the flammability and explosivity of nanopowders [4,20]. Normal exposure of non-pyrophoric metallic powders during handling operations and storage for a few days does not affect the explosivity of the nanopowder [20] whereas long-term storage of

aluminium nanopowders, even in an airtight container, can lead to an increase of the oxidation initiation temperature [27]. Further work performed by Boilard et al. [4] on nano-titanium also demonstrated that only high content of oxide, above 65%w., will influence the explosion severity of the powder.

Other studies deal with the production of relevant data on the flammability and explosivity of nanopowders for standardisation [28] and safety purposes [29]. It appeared that nano-titanium powder was much more sensitive to ignition than micro Ti powder in terms of fire hazards [30,31]. Such differences can be related to the major influence of heat and mass transfers on the combustion regime. Gao et al. [22] showed for 40 nm aluminum, titanium and iron particles that the combustion regime and phase (gas, liquid or solid) depend both on their chemical nature and their size.

It is then important to determine the actual particle size distribution of the dust cloud before its ignition. However, this distribution does not correspond to that obtained neither by wet laser diffraction, nor by only considering the primary particle sizes. Indeed, an in-depth understanding of the agglomeration of nanopowders is necessary to assess its influence on the explosion severity [32,33]. Thus, it is believed [29] that agglomeration deserves further attention to explain the decrease of explosion severity observed by some authors [34–36]. The effect of the turbulence of the dust cloud on its homogeneity and its explosivity should also be highlighted: increasing the flow turbulence has a stronger impact on aluminium nanopowders than on aluminium micro-powders explosivity [37].

So far, because of scarcity of data, safety data on nanosized powders tends to be compared directly to safety data on microsized powders with a principle of equivalence, without assessing in the discussion the true impact of the specific properties at nanoscale such as varying ignition temperatures, burning time, Knudsen limit etc. [22, 38]. To improve the current picture of the explosion course from nanosize to microsize, a database gathering

explosion safety parameters for several metallic materials was build and enriched with additional measurements of explosion severity of nanopowders. In a second part, the available data were analysed in order to describe the course of explosion behaviour from nanosize to microsize. Finally, an attempt has been made to highlight the detailed physico-chemical parameters that drive the explosion severity mainly by analysing flame propagation models and reconsidering the classical 'Kst approach' that is known to suffer from intrinsic theoretical limitations [39].

## 2. Selection and characterisation of nanodust metallic samples

Most of the experiments performed with metal nanoparticles and detailed in the literature have been carried out on aluminium, zinc, titanium, iron, magnesium or, less frequently, on copper. Titanium, iron and magnesium are known to be prone to pre-ignition, even pyrophoricity, when handled in the form of very fine powders. In order to perform additional measurements while avoiding such perturbation, experimental efforts were focused on six different fractions of aluminium and one fraction of zinc. Former investigations [6,8,36] have shown that nano-aluminium powders can be tested well in apparatuses like 20 L-sphere without showing pre-ignition behaviour like titanium or iron samples, up to a certain concentration [40]. Moreover, the database for micron scale aluminium is also very comprehensive. This allows a good comparison of results with nanometer and micrometer samples. As a consequence, aluminium dusts of different particle sizes from 18 nm to 150 nm have been chosen. Aluminium with mean particle sizes of 150, 90-110 and 50-70 nm came from the same supplier while the other samples were provided by another one. In addition to previous experiments obtained for nano zinc (90-150 nm) [7], another zinc dust with a smaller fraction (40-60 nm) was also chosen for this study.

In order to be able determining the distribution of the primary particle sizes as precisely as possible, the particle size distribution (PSD) was measured in liquid dispersion by means of Mastersizer 2000 from Malvern Instruments using the standard ISO 13320.

*Table 1: Particle size distribution characteristics of the nanopowders in liquid dispersion*

| **Sample** | **Dispersion time in min** | **Particle size distribution characteristics in µm** | | |
|---|---|---|---|---|
| | | **$d_{10}$** | **$d_{50}$** | **$d_{90}$** |
| **Aluminium:** λ= 633 nm (red): refractive index: 1.373, absorption 7.618 λ= 470 nm (blue): refractive index: 0.6838, absorption: 5.75 | | | | |
| **Aluminium 150 nm** | 3 | 0.34 | 1.10 | 4.68 |
| **Aluminium 130 nm** | 9 | 0.33 | 1.22 | 8.69 |
| **Aluminium 90-110 nm** | 3 | 0.31 | 0.94 | 5.21 |
| **Aluminium 50-70 nm** | 3 | 0.26 | 1.04 | 7.43 |
| **Aluminium 40-60 nm** | 11 | 0.22 | 0.46 | 1.07 |
| **Aluminium 18 nm** | 5 | 0.20 | 0.73 | 2.21 |
| **Zinc:** λ= 633 nm (red) / 470 nm (blue): refractive index: 2.008, Absorption 0.1 | | | | |
| **Zinc 40-60 nm** | 7 | 0.11 | 1.71 | 7.06 |

The aluminium dust samples (ca. 0.2 g) were introduced into 80 ml of a neutral aqueous dispersant solution containing 0.1 % by weight of Dolapix CE64. Isopropanol was used for zinc. Then, the suspension was dispersed with an external ultrasonic sonotrode (Sonoplus HD 2200 with Sonotrode VS 70 T – Bandelin, with max. 200 W HF-power). Pulsed ultrasound (50/50) with about 80 % of the maximum power was applied. Different sonication times were

used for the dispersion before conducting the particle measurements on 1 mL of the pre-dispersed solution. By considering the smallest obtainable $d_{50}$ values, the finest measured particle size distribution is then saved as the final result. After recording the scattered light data, the particle size distribution was calculated using the so-called Mie solution to Maxwell's equations using refractive index and adsorption (see Table 1).

In Table 1, it becomes obvious that median values of the agglomerates of all dust samples lie well above the given nanometre range. Due to high surface energy of nano-powders [41] all tested samples are subjected to attraction forces and tend to agglomerate, even under the best conditions in ultrasonic dispersion (low concentrations, ideal dispersing agent, etc.). It should also be underlined that, for aluminium samples, the $d_{10}$ values are in accordance with the primary particle size, i.e. the greater the primary particle size, the greater the $d_{10}$. The previous characteristics give some clues for understanding the agglomeration behaviour of nanoparticles but they do not correspond to the particle size distribution of the powder dispersed in air before a dust explosion. To understand dust properties under ambient conditions, particle size distribution in gas phase of the samples was therefore determined by laser diffraction (Mastersizer 2000). Dry dispersion was conducted with dispersion unit Scirocco 200 (Malvern Instruments) (Cf. Results in Table 2).

Characteristic diameters obtained with PSD measurements in liquid phase are lower than those obtained during the dry dispersion of the powders. Moreover, minimum values are observed for aluminium 50-70 nm, which can correspond to a deagglomeration optimum. Indeed, for very fine particles, the attractive and diffusional forces are significant which lead to contact and agglomeration, whereas for larger diameters, the collisional mechanisms and inertial forces are predominant in such structure growth [42]. Finally, it should be added that accurate determination of the particle size distribution of the dust cloud at the precise moment of its ignition can be obtained by performing in-situ analyses in the standardised vessels [40].

*Table 2: Particle size distribution characteristics of the nanopowders dispersed in gas phase*

| **Sample** | **Particle size distribution in µm** | | |
|---|---|---|---|
| | $d_{10}$ | $d_{50}$ | $d_{90}$ |
| **Aluminium 150 nm** | 0.82 | 6.76 | 163.72 |
| **Aluminium 130 nm** | 0.65 | 3.82 | 21.77 |
| **Aluminium 90-110 nm** | 0.64 | 4.90 | 15.11 |
| **Aluminium 50-70 nm** | 0.57 | 1.83 | 13.44 |
| **Aluminium 40-60 nm** | 0.83 | 6.16 | 14.62 |
| **Aluminium 18 nm** | 1.76 | 8.24 | 16.62 |
| **Zinc 40-60 nm** | 0.49 | 2.30 | 45.98 |

Determination of true density was conducted with gas pycnometer AccuPyc 1340 II (Micrometrics) with Helium 5.0 according to DIN 66137-2. All samples were dried for more than 20 hours at 50 °C (Cf. Results in table 4).

Measurements for the determination of the BET specific surface area were conducted with NOVA 2200 (Quantachrome) following ISO 9277 and ISO 185757 (five-points measurement).

A final overview of all characterisation results is also given in table 4. Furthermore, the moisture content of all samples was determined before testing according to Karl-Fischer method was conducted with a 756 KF calorimeter (oven type KF Thermoprep 832 - temperature of 150 °C). Measured values for BET surface area much smaller than theoretically possible surface areas, resulting from the sum of all single particles. It can be explained by the agglomeration of particles and the particle-particle contacts which limit the

adsorption surface. It is also likely that the whole inner surface area is not considered with the measurement.

*Table 3: Overview of characterisation results performed on Al and Zn nanopowders*

| **Sample** | **True density in g.cm$^{-3}$** | **$d_{50}$ in µm (liquid dispersion)** | **$d_{50}$ in µm (gas phase)** | **Specific surface area (BET) in m$^2$.g$^{-1}$** | **Moisture content in %** |
|---|---|---|---|---|---|
| **Aluminium** | | | | | |
| **150 nm** | 2.75 | 1.100 | 6.758 | 15.03 | 0.80 |
| **130 nm** | 2.74 | 1.222 | 3.819 | 12.45 | 0.65 |
| **90-110 nm** | 2.78 | 0.945 | 4.897 | 10.76 | 0.89 |
| **50-70 nm** | 2.81 | 1.038 | 1.831 | 13.68 | 0.88 |
| **40-60 nm** | 2.71 | 0.463 | 6.163 | 23.20 | 0.96 |
| **18 nm** | 3.00 | 0.728 | 8.240 | 22.34 | 1.85 |
| **Zinc** | | | | | |
| **40-60 nm** | 6.68 | 1.714 | 2.297 | 4.95 | 0.19 |

Measured densities of aluminium powders are all higher than the value found in literature [43] and the measured density for zinc is below the literature value. All samples have a thin oxide layer. It should be underlined that, based on the previous data and for Al nanoparticles ranging from 50 to 150 nm, calculations of the alumina layer thickness lead to values ranging from 0.7 to 1.2 nm, which is consistent with Sundaram et al. [26] who stated that aluminium nanoparticles with an oxide-layer thickness in the range of 0.5–4.0 nm are non-pyrophoric.

## 3. Results and discussion

### 3.1. Experimental evidences

The measurements of dust explosion severity, i.e. the maximum overpressure ($p_{max}$) and maximum rate of pressure rise $(dp/dt)_{max}$ were performed in the standardized 20 L explosion chamber [3]. The explosion sphere consists of a spherical combustion chamber made of stainless steel, a dust storage container connected with the chamber via a dust outlet valve, a pair of electrodes holding two pyrotechnic igniters of 5 kJ at the sphere centre and two pressure sensors to record the explosion development. The chamber is surrounded by a jacket with flowing cooling water to keep the chamber wall temperature constant from test to test. Maximum overpressure and maximum rate of pressure rise parameters are obtained through several tests with step-wise increase in dust concentration. The tests were performed according the EN 14034 series and the operating instructions of the 20 L-sphere [44].

Table 4 summarizes the explosion safety characteristics of the experimental tests performed in this study by BAM (*test performed by INERIS).

*Table 4. Explosion safety characteristics of nano-aluminium and nano-zinc samples*

| **Samples** | **Specific surface area (BET) in $m^2.g^{-1}$** | **$p_{max}$ (barg)** | **$(dp/dt)_{max}$ ($bar.s^{-1}$)** |
|---|---|---|---|
| **Aluminium 150 nm** | 15.03 | 10.2 | 2486 |
| **Aluminium 130 nm** | 12.03 | 7.8 | 1030 |
| **Aluminium 90-110 nm** | 10.76 | 7.9 | 1102 |
| **Aluminium 50-70 nm** | 13.68 | 8.3 | 1573 |
| **Aluminium 40-60 nm** | 23.20 | 8.9 | 2251 |
| **Aluminium 18 nm** | 22.34 | 7.3 (7.1*) | 564 (517*) |
| **Zinc 40-60 nm** | 4.95 | 5.9 | 869 |

In order to assess the course of explosion behaviour of metal powders and in addition to the previous experimental data, available literature data for microsized and nanosized metal powders were gathered in a comprehensive database. Results are illustrated graphically for 5 metallic powders, namely aluminium (Figures 1 and 2), magnesium (Figures 3 and 4), titanium (Figures 5 and 6), iron (Figures 7 and 8) and zinc (Figures 9 and 10). It should be stressed that the solid (or dotted) lines have been added to illustrate a tendency and do not correspond to a model or a curve fit. In some figures, an important dispersion of the experimental data is noticed, both for low and high specific surface areas. It should be kept in mind that this parameter has been determined either by BET measurements or by calculations based on mass median diameter and on the assumption of unimodal particle size distribution. Moreover, the specific surface area is not the only relevant parameter to consider when determining the explosion severity of a dust. Finally, the data collected were obtained under the same experimental conditions, following the same procedure. As well known, variations of the ignition energy, the ignition delay time (turbulence) or the explosion vessel shape can significantly impact the explosion severity.

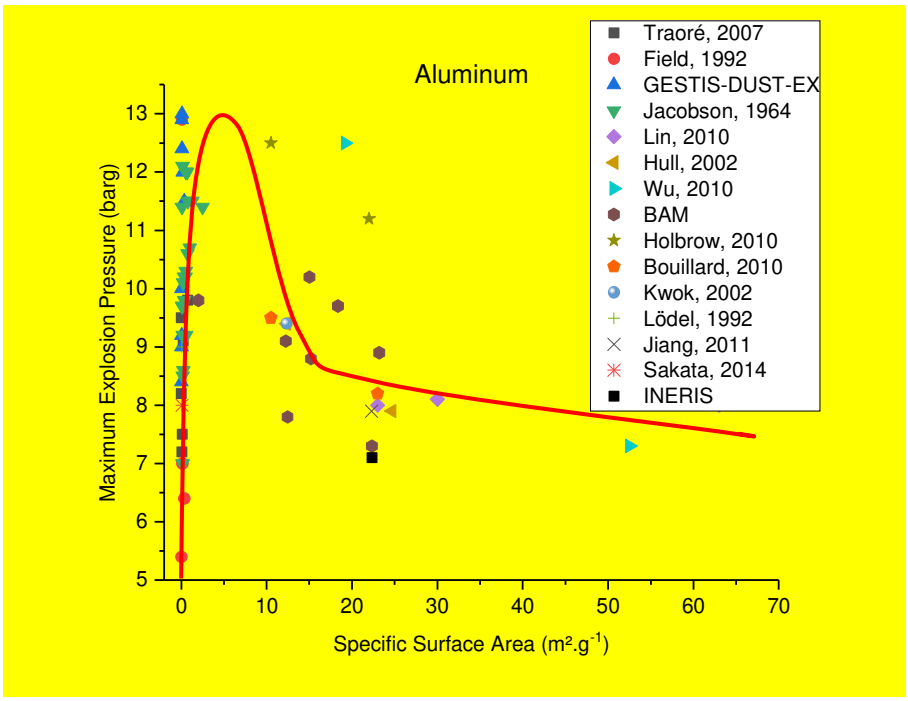


Figure 1. Evolution of the maximum explosion pressure of aluminium as a function of the specific surface area. Sources: data from BAM, INERIS, LRGP and [14,21,45–54]

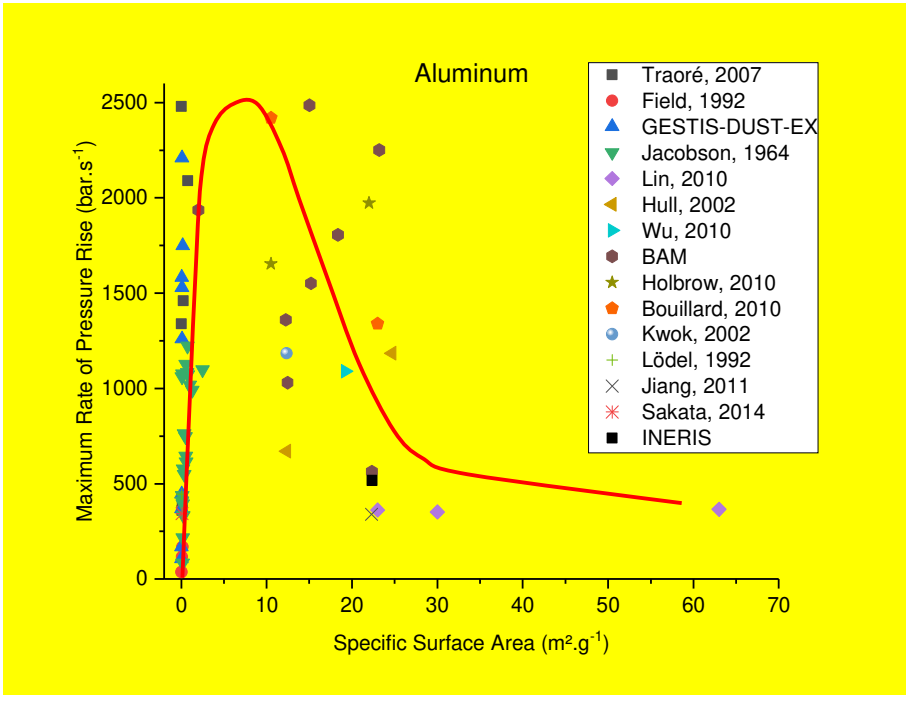


Figure 2. Evolution of the maximum rate of pressure rise of aluminium as a function of the specific surface area. Sources: data from BAM, INERIS, LRGP and [14,21,45–54]

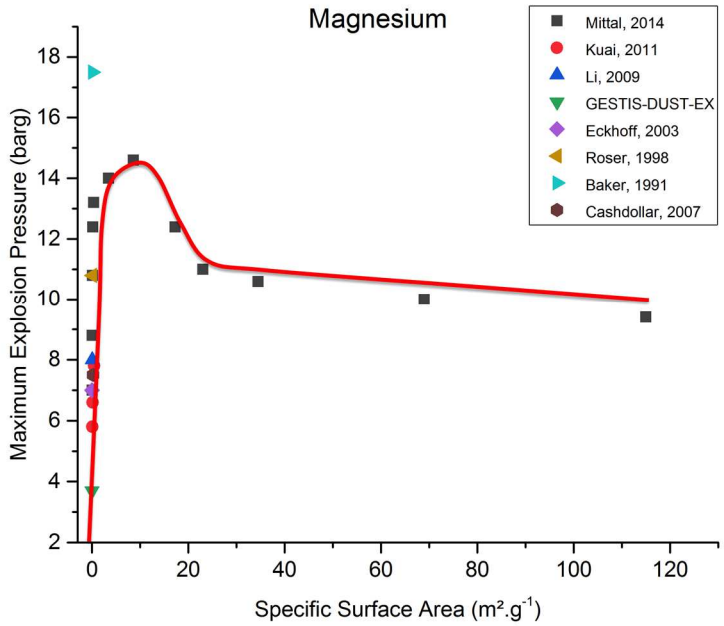


Figure 3. Evolution of the maximum explosion pressure $p_{max}$ of magnesium as a function of the specific surface area. Sources: data from [2,3,9,47,55–58]

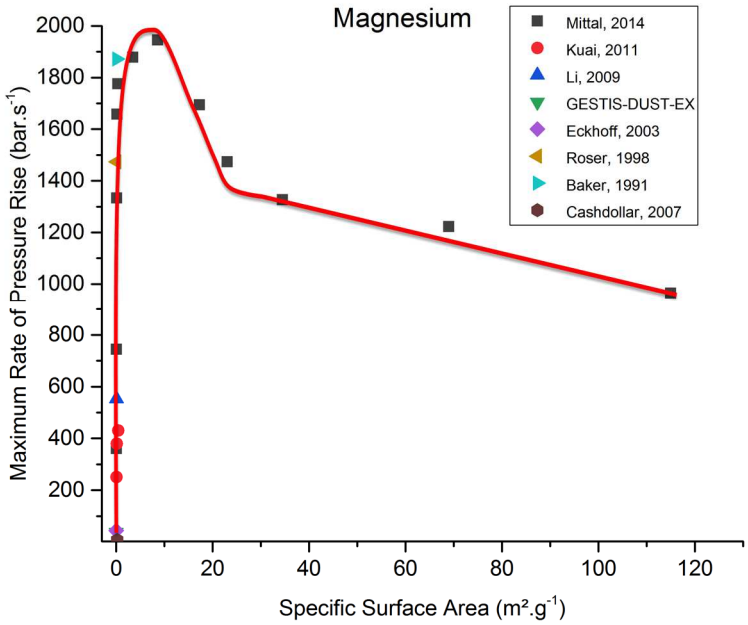

Figure 4. Evolution of the maximum rate of pressure rise $(dp/dt)_{max}$ of magnesium as a function of the specific surface area. Sources: data from [2,3,9,47,55–58]

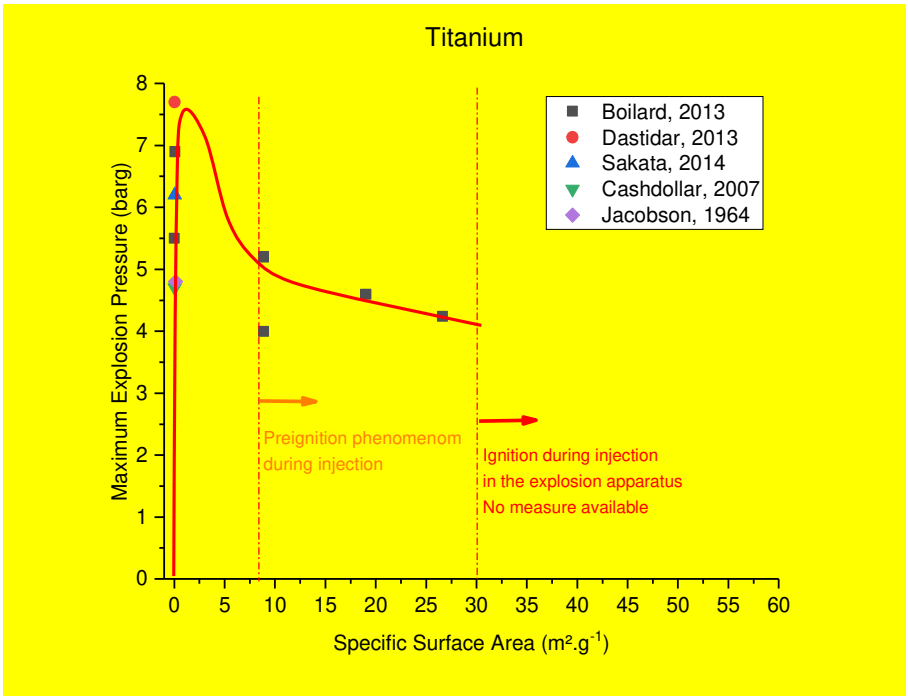


Figure 5. Evolution of the maximum explosion pressure $p_{max}$ of titanium as a function of the specific surface area. Sources: data from [2,4,5,48,54]

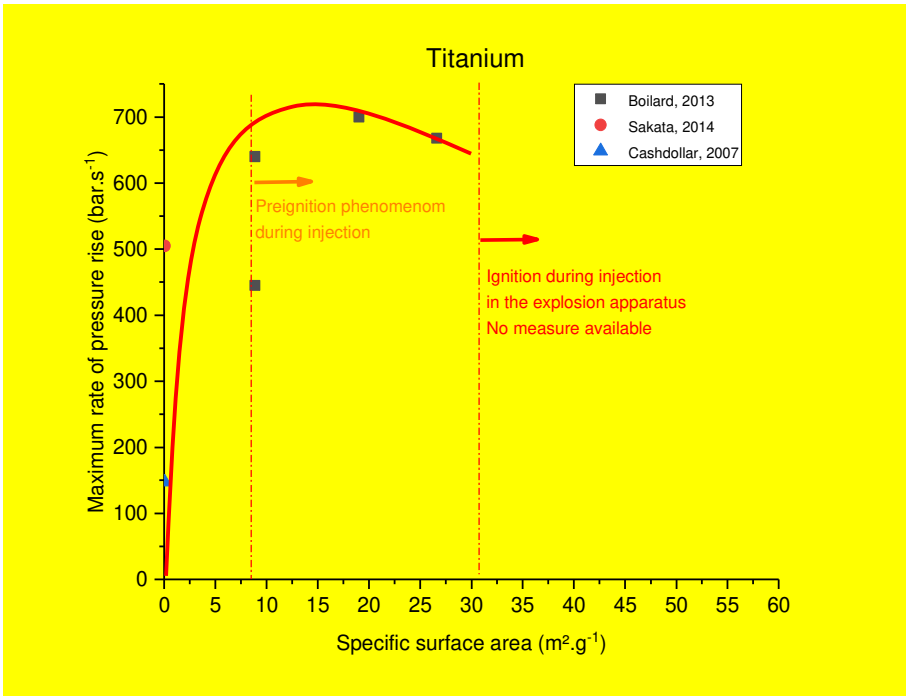

Figure 6. Evolution of the maximum rate of pressure rise $(dp/dt)_{max}$ of titanium as a function of the specific surface area. Sources: data from [2,4,54]

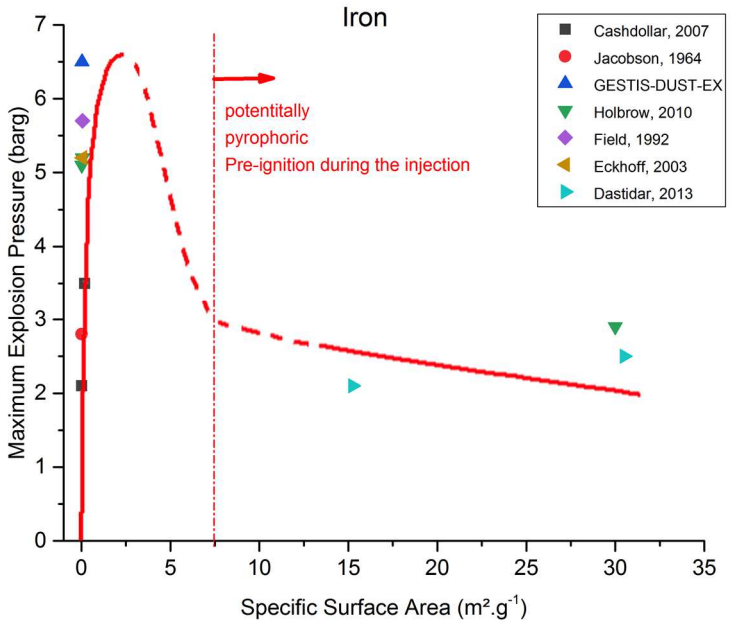


Figure 7. Evolution of the maximum explosion pressure $p_{max}$ of iron as a function of the specific surface area. Sources: data from [2,3,5,21,46–48]

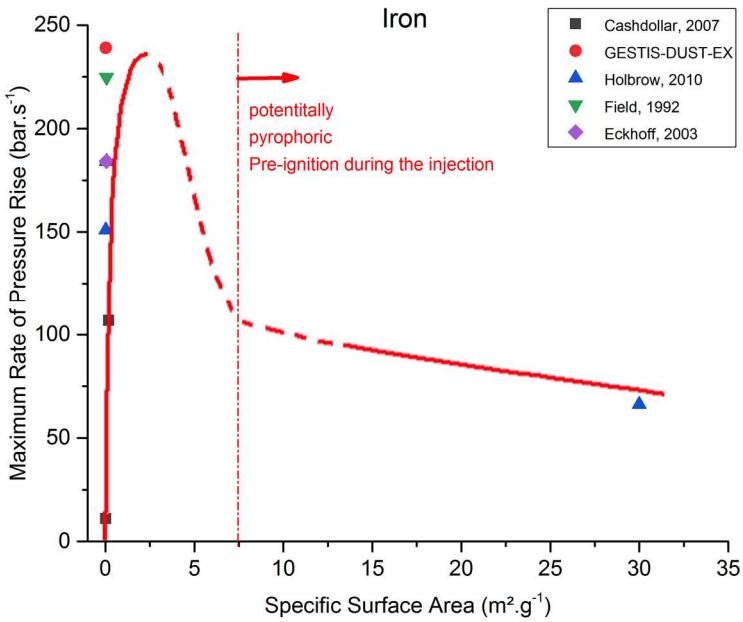

Figure 8. Evolution of the maximum rate of pressure rise $(dp/dt)_{max}$ of iron as a function of the specific surface area. Sources: data from [2,3,21,46,47]

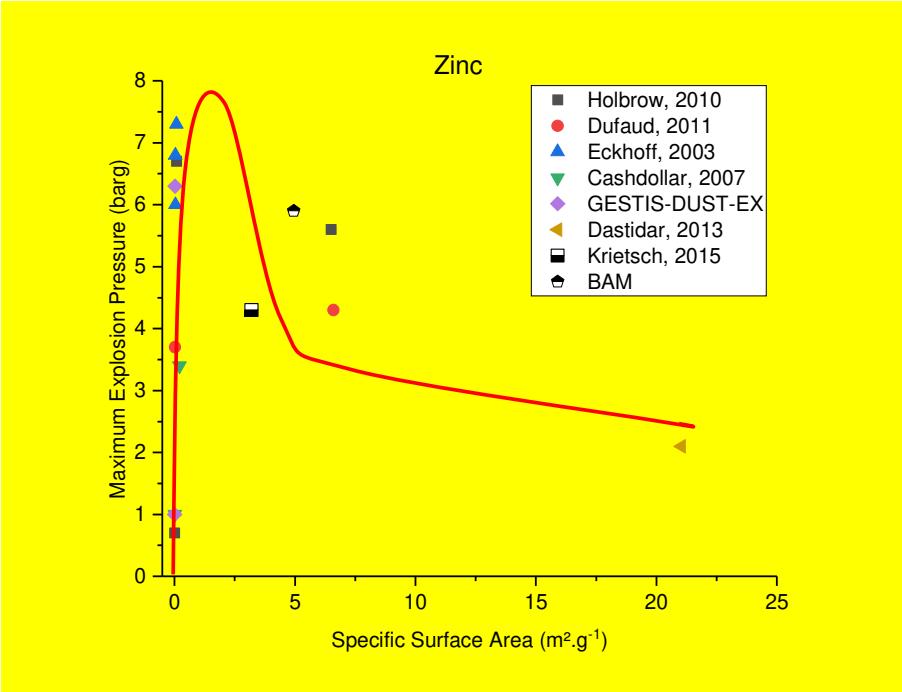


Figure 9. Evolution of the maximum explosion pressure $p_{max}$ of zinc as a function of the specific surface area. Sources: data from BAM, INERIS, LRGP and [2,3,5,7,21,47]

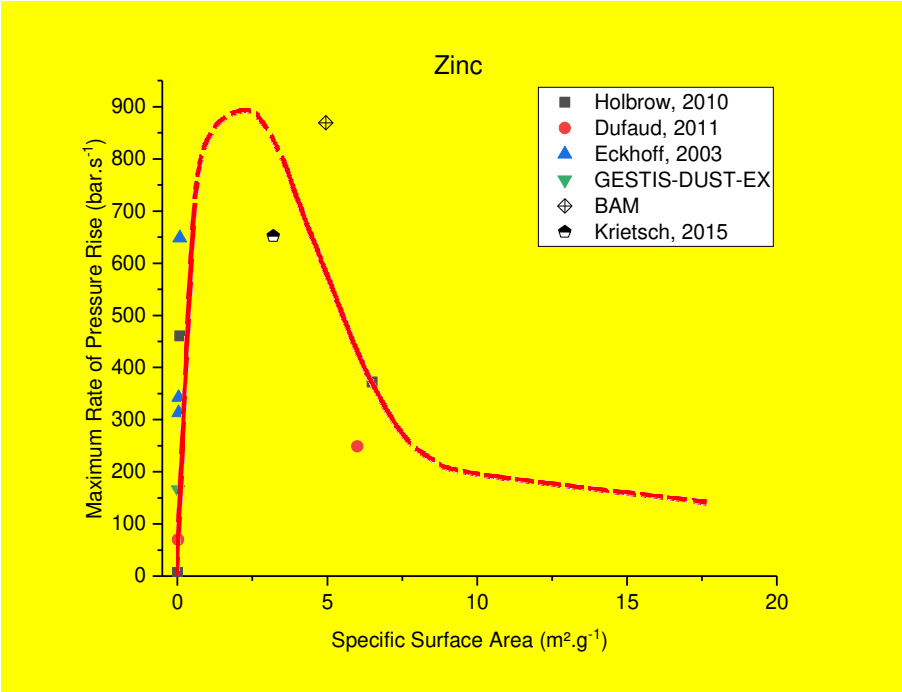

Figure 10. Evolution of the maximum rate of pressure rise $(dp/dt)_{max}$ of zinc as a function of the specific surface area. Sources: data from BAM, INERIS, LRGP and [3,7,21,47]

A specific pattern related to the evolution of explosivity (i.e. maximum explosion rate, maximum rate of pressure rise) is observed for the studied metallic materials. These figures show that the explosion severity of nanopowders is not systematically higher than that of microsized dusts and, notably due to agglomeration, tends to decrease with decreasing the particle size below a specific diameter. Due to a lack of data, similar statements cannot be outlined for other metals at the moment (for instance, zirconium or nickel). It should be also noted that in case of very reactive nanomaterials like titanium, iron or fine aluminium, the behaviour of explosion severity cannot be drawn entirely along the concentration range due to a so-called pre-ignition of nanopowders. Such phenomenon can be either due to the friction and shear forces applying on the particles during the injection into the explosion sphere or to pyrophoricity. Consequently, obtained safety parameters are not entirely representative of the original powder in such case.

The previous figures (1 to 10) clearly show that the metal nature greatly affects the maximum explosion pressure, and thus the maximum temperature reached inside the explosion vessel. The latter parameter and the combustion mechanism can be assessed, in a first approach, by considering the melting and boiling temperatures of the metals and their respective oxides (Table 6). By considering Glassman's criterion, i.e. comparing the dissociation or boiling temperature of the metal oxide with the boiling point of the metal, it appears that aluminium, iron, magnesium and zinc should burn in the vapour phase whereas titanium is prone to burn in a heterogeneous reaction. It should be underlined that the significance of this criterion was discussed, especially due to the lack of distinction between boiling and dissociation [59]. For a diffusion flame, as explained by Glassman et al. [60] the combustion temperature seems to

be limited by the boiling point of the metal oxide $T_{boil,oxi}$, due to the condensation of the oxidation products during their cooling, which is confirmed by comparing $T_{boil,oxi}$ and the experimental flame temperature $T_{f,exp}$ in Table 5. The combustion temperature is expected to be lower in the case of a heterogeneous reaction, as the kinetic is considered as the rate-limiting step. On these grounds, observing a maximum explosion pressure lower for titanium than for aluminium or magnesium is not surprising. However, as previously noted, many other parameters should be taken into account in order to interpret the experimental results.

It should also be underlined that the ignition process can be strongly different from the flame propagation process, and that the influence of surface phenomena, such as the protective oxide layer destruction, plays a major role when it comes to ignition [60]. As a consequence, the protective effect of the oxide layer has to be assessed through, for instance, the Pilling-Bedworth ratio (PBR), which is the ratio of the oxide created to the metal consumed [60–62]. When PBR is greater than unity, the oxide layer provides a protective effect and the ignition temperature is increased as oxygen and metal ions have to diffuse through it (Table 5). This is the case for iron, zinc, titanium and, to a lesser extent, aluminium. Considering this criterion, the ignition of magnesium is enhanced due to the presence of a thin/non-protective oxide layer (PBR lower than unity). However, PBR is not the only criterion to consider and the ignition energy or the specific surface area are also important parameters. Indeed, for high ignition energies or for small particles with a low radius of curvature (nanoparticles for instance), the thermal and mechanical stresses can be increased and cause the protective oxide film to break even for PBR greater than unity.

*Table 5. Melting, boiling, flame temperatures and Pilling and Bedworth ratio for the various metallic powders*

| Metal | $T_{melt,met}$ (K) | $T_{boil,met}$ (K) | $T_{melt,oxi}$ (K) | $T_{boil,oxi}$ (K) | Oxide | PBR | $T_{f,adia}$ (K) | $T_{f,exp}$ (K) |
|---|---|---|---|---|---|---|---|---|
| **Al** | 930 | 2720 | 2323 | 3800 | $Al_2O_3$ | 1.28 | 4060 | 2800 |
| **Fe** | 1811 | 3133 | 1650 | 3687 | FeO | 1.7 | 2490 | 1800 |
| **Mg** | 920 | 1370 | 3075 | 3350 | MgO | 0.81 | 3610 | 2800 |
| **Ti** | 2000 | 3530 | 2400 | 3300 | $Ti_2O_3$ | 1.73 | 3990 | 2850 |
| **Zn** | 693 | 1180 | 2248 | 2633 | ZnO | 1.58 | 2070 | 1750 |

The previous considerations are clearly insufficient to explain the variations observed in Figures 1 to 10 as they do not take the specificities of metal nanopowders into account. Firstly, the Glassman's criterion is based on the knowledge of the boiling/melting point of the metals and their oxides. However, the melting temperature of nanopowders depends on its diameter and tends to decrease when the particle size decreases, e.g. down to 1000 K for nano-Al [60]. It should be underlined that such deviation from a constant melting temperature observed for micropowders, is mainly observed for diameters lower than 20 nm . This trend, due to the cohesion energy of surface atoms which is lower than for interior atoms, induces that the ignition energy of metal nanopowders significantly decreases for small particle sizes [38]. On the contrary, the reactivity of nanopowders can be hindered by a relatively high oxide content. For instance, nano-Al particles have a 0.5 to 4 nm thick oxide layer, which is not greatly different from an aluminium microparticle [63]. In addition to their high specific surface area, surface defects can also have a great influence on the reactivity of metal nanoparticles [60]. Another aspect which has to be kept in mind for nanopowders is their mean free path in the gas phase. For Knudsen numbers Kn greater than unity (here for diameter lower than 130 nm), the continuum assumption is no longer valid, i.e. the powder

cannot be considered as macroparticle surrounded by a continuum of gas molecules [22]. Consequently, the mean free path is noticeably influenced by the temperature and pressure modifications and the combustion is kinetically controlled even for metals whose boiling temperature is lower than the vaporisation temperature of their oxide. Nevertheless, it should be noted that this transition from a continuum assumption to free molecular regime also influences the agglomeration process, particles with high Kn being more prone to coalescence and aggregation than agglomeration [64].

Another modification caused by the use of metallic nanoparticles is related to the optical properties of the reactive dust cloud. By combining Wien's law and the maximum flame temperatures calculated by using CEA code and shown in Table 5, it appears that the wavelength corresponding to the maximum radiance varies approximately from 1000 to 1660 nm. Then, the size parameter (or Mie parameter expressed as the ratio $2.\pi.r/\lambda$ with r the radius of the scattering particle and $\lambda$ the wavelength the of the incident radiation) x is lower than 0.2 for nanopowders having a mean diameter lower than 65 and 105 nm, respectively [65]. As a consequence, Rayleigh scattering has to be considered for small particles, which means that forward scattering is not as predominant as for micron-size particles and that preheating of the dust cloud located upstream of the flame will be different. It should be noted that the scattering effect will be negligible for x lower than $2.10^{-3}$, which is not the case for the metallic nanopowders considered here. Finally, by testing microsized or nanosized aluminium particles, significant modifications of the flame front radiation in the visible range were notably observed by Dufaud et al. [7]. The influence of the thermal transfer modes on the explosion severity can also be highlighted by considering various classical flame propagation models.

### 3.2. Flame propagation models

3.2.1. Application of Cassel's thermal theory

In order to give an interpretation about the role of the particle size on the explosion severity, the thermal theory of Cassel [66–68] relating flame velocity to the physico-chemical characteristic of burning particles has been considered in a form more general than the one originally developed by Cassel in order to facilitate the discussions:

$$\begin{cases} S_{UL} = K_2 + \sqrt{K_1 + K_2^2} \\ K_1 = \dfrac{1}{\tau_b} \cdot \dfrac{\lambda_g}{\left(C_{Pg}.\rho_g + C_{ps}.C_d\right)} \cdot \dfrac{\left(T_{ad} - T_{ign}\right)}{\left(T_{ign} - T_u\right)} \\ K_2 = \dfrac{\varepsilon_s.\sigma.F.}{2.\left(C_{Pg}.\rho_g + C_{ps}.C_d\right)} \cdot \dfrac{\left(T_{ad}^4 - T_u^4\right)}{\left(T_{ign} - T_u\right)} \end{cases} \quad (1)$$

Where $C_d$ is the mass concentration of dust in cloud, $C_{ps}$ specific heat of the particles, $C_{pg}$ the specific heat of air, $\delta_0$ the flame thickness, $T_{ad}$ the adiabatic flame temperature and $T_{ign}$ the ignition temperature of the particles, F the view factor of the flame front, which can be maximised to 1 for planar flames, $\boldsymbol{\tau_b}$ is the combustion time and σ the Boltzman constant. In this model, a planar flame is divided into two regions, a reaction zone and a preheat zone, and the temperature profile is assumed to be linear [69]. The $K_1$ term refers to the solution of this problem neglecting the contribution of heat radiation, which corresponds to the initial problem of Mallard and Le Chatelier; $K_2$ can be considered as the radiation contribution. If this model has been widely used to estimate the flame velocity of metal/air mixtures [70], it is clearly dependant on the determination (often, the arbitrary choice) of the ignition temperature $T_{ign}$.

Based on such a model, thermal radiation is expected to play an important role in laminar dust flame propagation. However, the role of thermal radiation is still unclear and rather controversial: some authors claim that radiation is a significant contributor to laminar flame propagation [7,67,70–72], rather than others concluded that radiation is not a significant

contributor [73–75]. Interesting discussions about pro and con were developed by Ogle [69]. Though some research teams are developing new modelling approaches to better understand the contribution of radiation to the laminar flame velocity [70,76–79], it should be kept in mind that currently the experimental investigations into the role of radiation are too much scarce to draw clear statements. Further experimental work should be carried out where particle size distribution, dust concentration and volume of equipment are carefully varied and controlled to explore various dust cloud configurations. By considering the work of Van de Hulst [80], which defines the extinction length of radiation in a cloud as:

$$\delta_R = \frac{2.\rho_s.d_p}{3.C_d} \qquad (2)$$

it can be stated basically that radiation will play an important role mostly for optically thick dust clouds, i.e. high dust concentrations of nanoparticles. However, this relation does not take the shape of the flame into consideration (planar, wrinkled…) and is based on Beer-Lambert's law whose applicability to such problems has been recently questioned [70]. However, it should be reminded that explosion results gained on nanopowders were obtained by performing tests at lab-scale, where the radiative contribution to flame propagation is minimised, mainly because of the convexity of the flame. In other words, the radiation contribution is scale dependant. Though this aspect was already known in the early 60's [67], investigations are still going on [81,82] to mitigate reliably large scale dust explosion of light metal dust.

Consequently, in a first approach and in order to interpret the course of metal dust explosion in a small-scale equipment, i.e. when the radiation is assumed to be negligible, the flame velocity should be expressed as:

$$S_{UL} = \sqrt{\frac{1}{\tau_b}.\frac{\lambda_g}{\left(C_{Pg}.\rho_g + C_{ps}.C_d\right)}.\frac{\left(T_{ad} - T_{ign}\right)}{\left(T_{ign} - T_u\right)}} \qquad (3)$$

Where $\tau_b$ is the combustion time (s). This relationship requires the determination of a combustion time. By considering a typical $d^n$ power law for the burning time and that the ignition temperature is independent from particle diameter, the flame velocity can be expressed as:

$$S_{UL} \propto \frac{1}{d_p^{n/2}} \qquad (4)$$

This relationship shows that as long as $T_{ign}$ does not vary with particle size, the flame velocity is mainly under the influence of the type of combustion regime (either kinetically or diffusionally driven). For a given concentration, the flame velocity will increase with smaller particle size, which is consistent with investigations on microsized particles [83].

In the case of metallic powders, ignition temperature is rather constant at microsize level and decreases with smaller particles sizes [84]. Typically, in the case of aluminium, Risha et al. [85] proposed an empirical relationship describing $T_{ign}$ as a function of particle size till 1 μm:

$$T_{ign} \propto d_p^{\gamma} \qquad (5)$$

With γ a constant. In the case of nanopowders, the burning time is usually under kinetic influence. For aluminium a more detailed empirical expression of the ignition temperature was proposed by other authors [86,87] and can be extended to metal nanoparticles as:

$$\tau_b = \frac{d_p^k}{A_1 . \exp\left(-\frac{A_2}{1 + A_3 T_{ign}}\right)} \qquad (6)$$

Where k value is theoretically 1 for organic powder and less than 1 for metallic powder (typically, k equals 0.3 in the case of aluminium) and $A_i$ some constants.

By replacing the $T_{ign}$ in the equation (5) and by considering that $T_{ign}$ is much greater than the temperature of unburnt mixture $T_u$, then the flame velocity can be expressed roughly as:

$$S_{UL} \propto d_p^{k/2} \exp\left(-\frac{1}{1+\alpha_1.d_p^k}\right)\sqrt{.1-\alpha_2.d_p^k} \qquad (7)$$

Where $\alpha_1$ and $\alpha_2$ are two constants

The derivative of this equation can be written as:

$$\frac{\partial S_{UL}}{\partial d_p} \propto \left(f\left(d_p\right)-g\left(d_p\right)\right).S_{UL} \qquad (8)$$

Where f and g are two positive functions depending on the diameter of particle. This expression shows for nanopowders under kinetic regime that the flame velocity will increase with decreasing particle size, until it reaches a maximum and then will start to decrease. This is typically the trend observed for the various metal powders in Figures 1 to 10. These statements show that, subject to the previous assumptions, the conductive thermal theory can be useful to model the explosion characteristics of nanopowders, provided that sufficient data are available as inputs.

It should be kept in mind that the statements hereafter are assumed to be relevant for light metal dust explosion in the 20 L explosion sphere (if the contribution of heat radiation is assumed to be negligible) and should not be extended to large scale. Though this model is rather simple, it is more phenomenological and is offering the opportunity to better understand the course of explosion behaviour of metallic powders at small scale. An interesting point about this model is that it considers ignition temperature as an input parameter, which varies with particle size [38]. It should be noted also that this model does not take into account any turbulence flow nor gravitational forces. In order to avoid the estimation of $T_{ign}$, other types of models were previously developed and are notably based on the assumption of an optically thick dust cloud [72].

2.2.2. Application of Huang's model

To go beyond the simplistic model of Cassel and get a confirmation of our assumptions, i.e. a flame propagation driven by combustion in the 20 L explosion sphere, the model developed by Huang et al. [88] has been considered by implementing all the available physico-chemical data on aluminium. This model consists in solving an algebraic equation depending on the physico-chemical properties of the particles as well as on the laminar flame velocity.

As before, the physico-chemical properties are calculated at an average combustion temperature and the combustion time at ignition temperature $T_{ign}$. The modelling results were compared to experimental available ones, i.e. data gained from direct measurements of flame velocity performed either with a "Bunsen" apparatus [67,71,85], a propagation tube [89] or the standard explosion sphere, as it was the case in this current work [6,8].

Several additional points should be noted. On the one hand, measurements with Bunsen apparatus or propagation tube are scarce because they are very difficult to be performed (e.g. no standardised approach, tests only performed by few researchers, no consensus on to set-up the facilities). In these conditions, discrepancies in data are intrinsic, but recent works have greatly improved such techniques [90–94].

On the other hand, concerning data gained by explosion experiments in a closed vessel, no flame velocity is directly measured for nanopowders but only safety parameters, i.e. explosion pressure and rate of pressure rise. So far, there is no acknowledged approach to link these data to flame velocity (actually the parameter of interest for comparison with modelling results). However, through a mass balance and parametric analysis [95,96], managed to combine these safety parameters to laminar flame velocity at ambient conditions such as:

$$S_L = a_{lam}.\frac{\left(\frac{dP}{dt}\right)_m.V^{1/3}}{\left(P_m - P_0\right).\left(\frac{P_m}{P_0}\right)^{1/\gamma+n}} \qquad (9)$$

Where $a_{lam}$ is a factor of proportionality which has been set at 0.11 by the authors by making a comprehensive analysis of the experimental measurements of flame velocity available in the literature. V the volume of the container in which the explosion propagates, $t_1$ is the time delay between the start of the explosion and the time at which the pressure reaches $P_m$, the maximum explosion pressure. Moreover, $\gamma$ and n are factors specific to the gas and the dust.

Comparison between available experimental results and modelling results obtained thanks to Huang's model were carried out at a concentration of 250 $g.m^{-3}$ at which there was a maximum amount of data. Experimental laminar flame velocities derived from the explosion measurements on aluminium were gathered in Table 6.

*Table 6. Experimental equivalent laminar flame velocity $S_L$ derived from the explosion measurements of aluminium at 250 $g.m^{-3}$*

| **Samples** | **$p_m$ (barg)** | **$(dp/dt)_m$ ($bar.s^{-1}$)** | **$S_L$(m/s)** |
|---|---|---|---|
| **Aluminium 150 nm** | 7.9 | 772 | 0.45 |
| **Aluminium 130 nm** | 5.6 | 398 | 0.42 |
| **Aluminium 90-110 nm** | 6.4 | 403 | 0.34 |
| **Aluminium 50-70 nm** | 5.4 | 215 | 0.24 |
| **Aluminium 40-60 nm** | 6 | 348 | 0.33 |
| **Aluminium 18 nm** | 2.9 | 70 | 0.22 |

Figure 11 suggests that flame propagation mode by conduction can explain quite quantitatively the experimental pattern observed for aluminium (and that is quite similar for other metals), at least for lean concentration. However, it should be stressed that if radiation contribution can be neglected for pure and individualized nanoparticles, such ideal situation is

seldom encountered in real/industrial situations, with high dust loadings leading to nanoparticles agglomeration. Therefore, radiation will increase the flame thickness, whereas the validity of the classical 'Kst approach' is restricted to dust clouds burning with thin flames [39]. Another limitation of the previous models is related to the assumption of the unimodal particle size distribution of spherical powders, which is obviously not the case with nanoparticles prone to agglomeration. Finally, the 'key role of turbulence' [39] and especially the evolution of the particle size distribution as a function of the turbulence (both agglomeration and fragmentation phenomena) should also be taken into account.

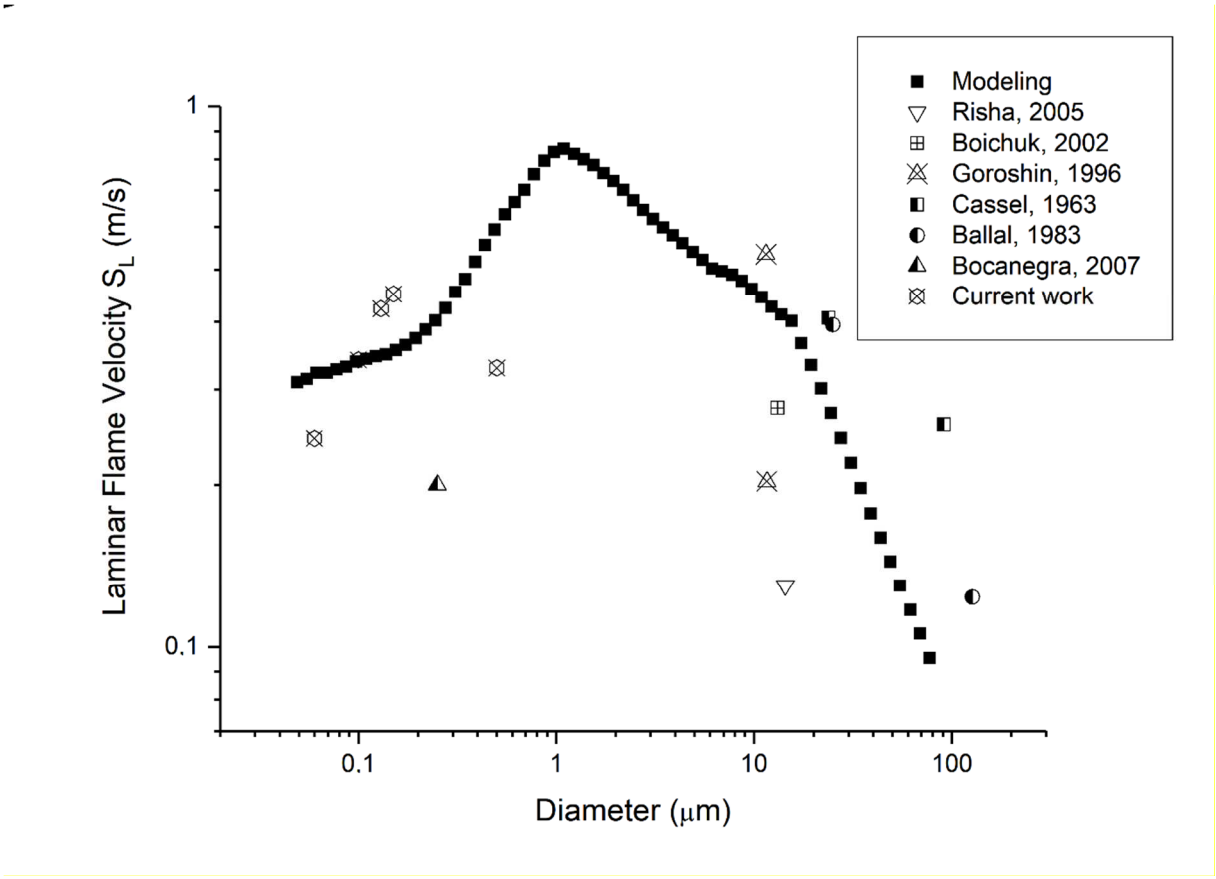


Figure 11. Evolution of the laminar flame velocity as a function of particle diameter (concentration of 250 $g.m^{-3}$)

## 4. Conclusion

The analysis of original experimental results and data from the literature clearly demonstrates that the explosion of metal powders is not necessarily more severe when the primary particle size decreases. Several criteria explaining this trend must be taken into consideration, starting with the natural propensity of nanopowders to agglomerate. However, other physico-chemical parameters should be taken into account, notably those related to the heat transfer phenomena (conductive or radiative) during the flame propagation. So, if agglomeration is neglected, the specific pattern observed in this study for metal nanopowders can clearly be related to the characteristics of a dust flame propagation driven by conduction. Such considerations about nanopowders agglomeration and the heat transfer modes of their flames are essential because they have direct practical repercussions on the extrapolation of safety parameters and on vent sizing.

## 5. Acknowledgements

This work was supported financially by the French Ministry of Environment, Ecology and Durable Development, the German Federal Ministry of Economic Affairs and Energy (TNS-Project contract N°03FS13035), the European Commission Seventh Framework Program Project FP7-MARINA (Grant N°263215 - www.marina.eu), and the European Commission Mandate M461 for standardization.

## 6. References

[1] J.M. Benson, Safety consideration when handling metal powders, J. South. Afr. Inst. Min. Metall. 7A (2012) 563–575.

[2] K.L. Cashdollar, I.A. Zlochower, Explosion temperatures and pressures of metals and other elemental dust clouds, J. Loss Prev. Process Ind. 20 (2007) 337–348. doi:10.1016/j.jlp.2007.04.018.

[3] R.K. Eckhoff, Dust Explosions in the Process Industries, Elsevier, 2003.

doi:10.1016/B978-0-7506-7602-1.X5000-8.

[4] S.P. Boilard, P.R. Amyotte, F.I. Khan, A.G. Dastidar, R.K. Eckhoff, Explosibility of micron- and nano-size titanium powders, J. Loss Prev. Process Ind. 26 (2013) 1646–1654. doi:10.1016/j.jlp.2013.06.003.

[5] A.G. Dastidar, S.P. Boilard, P.R. Amyotte, L. Turkevitch, 2013 aiche spring meeting & 9th global congress on process safety: conference proceedings., in: Amer Inst Of Chem Enginee, New York, 2013.

[6] J. Bouillard, A. Vignes, O. Dufaud, L. Perrin, D. Thomas, Ignition and explosion risks of nanopowders, J. Hazard. Mater. 181 (2010) 873–880.

[7] O. Dufaud, A. Vignes, F. Henry, L. Perrin, J. Bouillard, Ignition and explosion of nanopowders: something new under the dust, J. Phys. Conf. Ser. 304 (2011) 012076. doi:10.1088/1742-6596/304/1/012076.

[8] A. Krietsch, M. Scheid, M. Schmidt, U. Krause, Explosion behaviour of metallic nano powders, J. Loss Prev. Process Ind. 36 (2015) 237–243. doi:10.1016/j.jlp.2015.03.016.

[9] M. Mittal, Explosion characteristics of micron- and nano-size magnesium powders, J. Loss Prev. Process Ind. 27 (2014) 55–64. doi:10.1016/j.jlp.2013.11.001.

[10] SWA, Evaluation of potential safety (physicochemical) hazards associated with the use of engineered nanomaterials, (2013) 58.

[11] A. Vignes, F. Muñoz, J. Bouillard, O. Dufaud, L. Perrin, A. Laurent, D. Thomas, Risk assessment of the ignitability and explosivity of aluminum nanopowders, Process Saf. Environ. Prot. 90 (2012) 304–310. doi:10.1016/j.psep.2011.09.008.

[12] S.M. Worsfold, P.R. Amyotte, F.I. Khan, A.G. Dastidar, R.K. Eckhoff, Review of the Explosibility of Nontraditional Dusts, Ind. Eng. Chem. Res. 51 (2012) 7651–7655. doi:10.1021/ie201614b.

[13] H.-C. Wu, R.-C. Chang, H.-C. Hsiao, Research of minimum ignition energy for nano Titanium powder and nano Iron powder, J. Loss Prev. Process Ind. 22 (2009) 21–24. doi:10.1016/j.jlp.2008.10.002.

[14] H.-C. Wu, H.-J. Ou, H.-C. Hsiao, T.-S. Shih, Explosion Characteristics of Aluminum Nanopowders, Aerosol Air Qual. Res. 10 (2010) 38–42. doi:10.4209/aaqr.2009.06.0043.

[15] H.-C. Wu, H.-J. Ou, D.-J. Peng, H.-C. Hsiao, C.-Y. Gau, T.-S. Shih, Dust Explosion Characteristics of Agglomerated 35 nm and 100 nm Aluminum Particles, Int. J. Chem. Eng. (2010). doi:10.1155/2010/941349.

[16] H.-C. Wu, Y.-C. Kuo, Y. Wang, C.-W. Wu, H.-C. Hsiao, Study on safe air transporting velocity of nanograde aluminum, iron, and titanium, J. Loss Prev. Process Ind. 23 (2010) 308–311. doi:10.1016/j.jlp.2009.11.002.

[17] H.-C. Wu, C.-W. Wu, Y.-H. Ko, Flame phenomena in nanogrinding process for titanium and iron, J. Loss Prev. Process Ind. 27 (2014) 114–118. doi:10.1016/j.jlp.2013.11.002.

[18] ASTM E1226 – 12a, Standard Test Method for Pressure and Rate of Pressure Rise for Combustible Dusts, Annu. Book ASTM Stand. (2012) 1–13.

[19] European Committee for Standardisation, Determination of explosion characteristics of dust clouds, 2011.

[20] A. Krietsch, T.-M. Romahn, M. Scheid, U. Krause, Modified Setup of 20-L-Sphere for the Determination of Safety Characteristics of Nano Powders, Chem. Eng. Trans. 31 (2013).

[21] P. Holbrow, M. Wall, E. Sanderson, D. Bennett, W. Rattigan, R. Bettis, D. Gregory, Fire and explosion properties of nanopowders, UK Health and Safety, Executive, 2010. http://www.hse.gov.uk/research/rrhtm/rr782.htm (accessed February 24, 2019).

[22] W. Gao, X. Zhang, D. Zhang, Q. Peng, Q. Zhang, R. Dobashi, Flame propagation

behaviours in nano-metal dust explosions, Powder Technol. 321 (2017) 154–162. doi:10.1016/j.powtec.2017.08.013.

[23] S.W. Chung, E.A. Guliants, C.E. Bunker, P.A. Jelliss, S.W. Buckner, Size-dependent nanoparticle reaction enthalpy: Oxidation of aluminum nanoparticles, J. Phys. Chem. Solids. 72 (2011) 719–724. doi:10.1016/j.jpcs.2011.02.021.

[24] A. Ermoline, E.L. Dreizin, Equations for the Cabrera–Mott kinetics of oxidation for spherical nanoparticles, Chem. Phys. Lett. 505 (2011) 47–50. doi:10.1016/j.cplett.2011.02.022.

[25] S. Mohan, M.A. Trunov, E.L. Dreizin, On possibility of vapor-phase combustion for fine aluminum particles, Combust. Flame. 156 (2009) 2213–2216. doi:10.1016/j.combustflame.2009.08.007.

[26] D.S. Sundaram, P. Puri, V. Yang, Pyrophoricity of nascent and passivated aluminum particles at nano-scales, Combust. Flame. 160 (2013) 1870–1875. doi:10.1016/j.combustflame.2013.03.031.

[27] A. Ilyin, D. Tikhonov, A. Mostovshchikov, Parameters of Aluminum Nanopowders Activity after Long-Term Storage in an Airtight Container, Propellants Explos. Pyrotech. 43 (2018) 749–753. doi:10.1002/prep.201800178.

[28] J. Porcher, A. Vignes, B. Debray, A. Janes, D. Carson, E. Fréjafon, CEN/TC 352/WG3/PG3 – Protocols for determining the explosivity and Flammability of Powders Containing Nano-objects (for transport, handling and storage), in: Grenoble, France, 2014.

[29] P.R. Amyotte, Some myths and realities about dust explosions, Process Saf. Environ. Prot. 92 (2014) 292–299. doi:10.1016/j.psep.2014.02.013.

[30] C. Yuan, K. Liu, P. Amyotte, C. Li, J. Cai, F. Wang, G. Li, Electric spark ignition sensitivity of nano and micro Ti powder layers in the presence of inert nano TiO 2

powder, J. Loss Prev. Process Ind. 46 (2017) 84–93. doi:10.1016/j.jlp.2017.01.022.

[31] Y. Chunmiao, P.R. Amyotte, M.N. Hossain, C. Li, Minimum ignition energy of nano and micro Ti powder in the presence of inert nano TiO2 powder, J. Hazard. Mater. 274 (2014) 322–330. doi:10.1016/j.jhazmat.2014.04.007.

[32] J. Bouillard, F. Henry, P. Marchal, Rheology of powders and nanopowders through the use of a Couette four-bladed vane rheometer: flowability, cohesion energy, agglomerates and dustiness, J. Nanoparticle Res. 16 (2014) 2558. doi:10.1007/s11051-014-2558-0.

[33] F. Henry, J. Bouillard, P. Marchal, A. Vignes, O. Dufaud, L. Perrin, Exploring a new method to study the agglomeration of powders: Application to nanopowders, Powder Technol. 250 (2013) 13–20. doi:10.1016/j.powtec.2013.08.010.

[34] R.K. Eckhoff, Does the dust explosion risk increase when moving from µm-particle powders to powders of nm-particles?, J. Loss Prev. Process Ind. 25 (2012) 448–459.

[35] R.K. Eckhoff, Influence of dispersibility and coagulation on the dust explosion risk presented by powders consisting of nm-particles, Powder Technol. 239 (2013) 223–230.

[36] A. Vignes, Evaluation of ignition and explosion risks of nanopowders: a great way to manage industrial safety risks - Évaluation de l'inflammabilité et de l'explosivité des nanopoudres : une démarche essentielle pour la maîtrise des risques, PhD thesis (In French), Vandoeuvre-les-Nancy, INPL, 2008. http://www.theses.fr/2008INPL043N (accessed February 24, 2019).

[37] X. Liu, Q. Zhang, Influence of turbulent flow on the explosion parameters of micro- and nano-aluminum powder–air mixtures, J. Hazard. Mater. 299 (2015) 603–617. doi:10.1016/j.jhazmat.2015.07.068.

[38] D.S. Sundaram, P. Puri, V. Yang, A general theory of ignition and combustion of

nano- and micron-sized aluminum particles, Combust. Flame. 169 (2016) 94–109. doi:10.1016/j.combustflame.2016.04.005.

[39] R.K. Eckhoff, Use of (dP/dt)max from closed-bomb tests for predicting violence of accidental dust explosions in industrial plants, Fire Saf. J. 8 (1985) 159–168. doi:10.1016/0379-7112(85)90053-0.

[40] A. Santandrea, S. Pacault, L. Perrin, A. Vignes, O. Dufaud, Nanopowders explosion: influence of the dispersion characteristics, in: Kansas City, USA, 2018: p. 16.

[41] M. Seipenbusch, P. Toneva, W. Peukert, A.P. Weber, Impact Fragmentation of Metal Nanoparticle Agglomerates, Part. Part. Syst. Charact. 24 (2007) 193–200. doi:10.1002/ppsc.200601089.

[42] P. Meakin, A Historical Introduction to Computer Models for Fractal Aggregates, J. Sol-Gel Sci. Technol. 15 (1999) 97–117. doi:10.1023/A:1008731904082.

[43] R. Kaltofen, Tabellenbuch Chemie, 13th ed., Europa-Lehrmittel, 1998.

[44] C. Cesana, R. Siwek, Operating instructions 20-l-apparatus 6.0, Adolf Kühner AG, Switzerland: CH-4127 Birsfelden, 2001.

[45] M. Traore, Explosions de poussières et de mélanges hybrides : étude paramétrique et relation entre la cinétique de combustion et la violence de l'explosion, thesis, Vandoeuvre-les-Nancy, INPL, 2007. http://www.theses.fr/2007INPL019N (accessed February 24, 2019).

[46] P. Field, Dust Explosion - Handbook of Powder Technology, Elsevier, Amsterdam, 1992. https://www.elsevier.com/books/book-series/handbook-of-powder-technology (accessed February 24, 2019).

[47] BGIA, Combustion and explosion characteristics of dusts (BIA-Report 13/97) and Gestis Database, HVBG, Sankt Augustin, Germany, 1997.

[48] M. Jacobson, A.R. Cooper, J. Nagy, Explosibility of Metal Powders, Bureau of Mines,

1964.

[49] B.-Q. Lin, W.-X. Li, C.-J. Zhu, H.-L. Lu, Z.-G. Lu, Q.-Z. Li, Experimental investigation on explosion characteristics of nano-aluminum powder—air mixtures, Combust. Explos. Shock Waves. 46 (2010) 678–682. doi:10.1007/s10573-010-0089-2.

[50] M. Hull, Company Profile: Tetronics: plasma processing holds key to consistent nanopowders, Powder Metall. 45 (2002) 8–9. doi:10.1179/pom.2002.45.1.8.

[51] Q.S.M. Kwok, R.C. Fouchard, A.-M. Turcotte, P.D. Lightfoot, R. Bowes, D.E.G. Jones, Characterization of Aluminum Nanopowder Compositions, Propellants Explos. Pyrotech. 27 (2002) 229–240. doi:10.1002/1521-4087(200209)27:4<229::AID-PREP229>3.0.CO;2-B.

[52] R. Lodel, Incendies et explosions de métaux en poudre, INERIS, 1992.

[53] B. Jiang, B. Lin, S. Shi, C. Zhu, W. Li, Explosive characteristics of nanometer and micrometer aluminum-powder, Min. Sci. Technol. China. 21 (2011) 661–666.

[54] K. Sakata, K. Tagomori, N. Sugiyama, S. Sasaki, Y. Shinya, T. Nanbu, Y. Kawashita, I. Narita, K. Kuwatori, T. Ikeda, R. Hara, H. Miyahara, Dust Explosion Characteristics of Aluminum, Titanium, Zinc, and Iron-Based Alloy Powders Used in Cold Spray Processing, J. Therm. Spray Technol. 23 (2014) 123–130. doi:10.1007/s11666-013-0043-4.

[55] N. Kuai, J. Li, Z. Chen, W. Huang, J. Yuan, W. Xu, Experiment-based investigations of magnesium dust explosion characteristics, J. Loss Prev. Process Ind. 24 (2011) 302–313. doi:10.1016/j.jlp.2011.01.006.

[56] G. Li, C.M. Yuan, Y. Fu, Y.P. Zhong, B.Z. Chen, Inerting of magnesium dust cloud with Ar, N2 and CO2, J. Hazard. Mater. 170 (2009) 180–183. doi:10.1016/j.jhazmat.2009.04.121.

[57] M. Roser, Investigation of dust explosion phenomena in interconnected process vessels, PhD thesis, Loughborough University, 1998. https://dspace.lboro.ac.uk/dspace-

jspui/handle/2134/11692 (accessed February 25, 2019).

[58] W.E. Baker, M.J. Tang, Gas, dust, and hybrid explosions, Elsevier, 1991.

[59] T.A. Steinberg, D.B. Wilson, F. Benz, The combustion phase of burning metals, Combust. Flame. 91 (1992) 200–208. doi:10.1016/0010-2180(92)90100-4.

[60] I. Glassman, R.A. Yetter, N.G. Glumac, Combustion, Elsevier, 2015. doi:10.1016/C2011-0-05402-9.

[61] C. Xu, W. Gao, Pilling-Bedworth ratio for oxidation of alloys, (2000) 5.

[62] J.S. Dunn, The High Temperature Oxidation of Metals, Proc. R. Soc. Math. Phys. Eng. Sci. 111 (1926) 203–209. doi:10.1098/rspa.1926.0062.

[63] D.S. Sundaram, V. Yang, V.E. Zarko, Combustion of nano aluminum particles (Review), Combust. Explos. Shock Waves. 51 (2015) 173–196. doi:10.1134/S0010508215020045.

[64] A. D'Anna, Particle inception and growth: Experimental evidences and a modelling attempt, in: Combust. Gener. Fine Carbonaceous Part., Karlsruhe University Press, Bockhorn H, D'Anna A, Sarofim AF, Wang H (eds), Karlsruhe, 2009: pp. 289–320. https://www.researchgate.net/publication/291786535_Particle_inception_and_growth_Experimental_evidences_and_a_modelling_attempt (accessed February 25, 2019).

[65] V.I. Kostylev, Scattering Fundamentals, in: Bistatic Radar, John Wiley & Sons, Ltd, 2007: pp. 193–223. doi:10.1002/9780470035085.ch10.

[66] H.M. Cassel, A.K. Das Gupta, S. Guruswamy, Factors affecting flame propagation through dust clouds, Symp. Combust. Flame Explos. Phenom. 3 (1948) 185–190. doi:10.1016/S1062-2896(49)80024-9.

[67] H.M. Cassel, U.S.B. of Mines, Some fundamental aspects of dust flames, U.S. Dept. of the Interior, Bureau of Mines, 1964.

[68] H.M. Cassel, I. Liebman, W.K. Mock, Radiative transfer in dust flames, Symp. Int.

Combust. 6 (1957) 602–605. doi:10.1016/S0082-0784(57)80081-2.

[69] R.A. Ogle, Dust Explosion Dynamics, Elsevier, 2017. doi:10.1016/C2014-0-03833-6.

[70] C. Proust, B.M. Rim, G. Mohamed, S. Khashayar, F. Jérôme, Thermal radiation in dust flame propagation, J. Loss Prev. Process Ind. 49 (2017) 896–904. doi:10.1016/j.jlp.2017.01.002.

[71] Ballal D. R., Gaydon Alfred Gordon, Flame propagation through dust clouds of carbon, coal, aluminium and magnesium in an environment of zero gravity, Proc. R. Soc. Lond. Math. Phys. Sci. 385 (1983) 21–51. doi:10.1098/rspa.1983.0003.

[72] R.A. Ogle, J.K. Beddow, A.F. Vetter, L.-D. Chen, A thermal theory of laminar premixed dust flame propagation, Combust. Flame. 58 (1984) 77–79. doi:10.1016/0010-2180(84)90081-6.

[73] C. PROUST, B. VEYSSIERE, Fundamental Properties of Flames Propagating in Starch Dust-Air Mixtures, Combust. Sci. Technol. 62 (1988) 149–172. doi:10.1080/00102208808924007.

[74] C. Proust, Flame propagation and combustion in some dust-air mixtures, J. Loss Prev. Process Ind. 19 (2006) 89–100. doi:10.1016/j.jlp.2005.06.026.

[75] S. Goroshin, I. Fomenko, J.H.S. Lee, Burning velocities in fuel-rich aluminum dust clouds, Symp. Int. Combust. 26 (1996) 1961–1967. doi:10.1016/S0082-0784(96)80019-1.

[76] R. Ben Moussa, Contribution to thermal radiation to dust flame propagation : application to aluminium dust explosions, PhD thesis (in English), Compiègne, 2017. http://www.theses.fr/2017COMP2401 (accessed February 25, 2019).

[77] M.F. Ivanov, A.D. Kiverin, M.A. Liberman, Influence of radiation absorption by microparticles on the flame velocity and combustion regimes, J. Exp. Theor. Phys. 121

(2015) 166–178. doi:10.1134/S1063776115080063.

[78] D. Torrado, Effect of carbon black nanoparticles on the explosion severity of gas mixtures, PhD thesis (in English), Université de Lorraine, 2017. http://www.theses.fr/2017LORR0199 (accessed February 25, 2019).

[79] D. Torrado, A. Pinilla, M. Amin, C. Murillo, F. Munoz, P.-A. Glaude, O. Dufaud, Numerical study of the influence of particle reaction and radiative heat transfer on the flame velocity of gas/nanoparticles hybrid mixtures, Process Saf. Environ. Prot. 118 (2018) 211–226. doi:10.1016/j.psep.2018.06.042.

[80] H.C. Hulst, H.C. van de Hulst, Light Scattering by Small Particles, Courier Corporation, 1981.

[81] K. van Wingerden, S. Davis, G. As, Scaling of Metal Dust Explosions, in: Texas A&M Eng. Exp. Station, Texas, USA, 2014: p. 1.

[82] K. van Wingerden, S. Davis, Unknown Aspects of Metal Dust Explosions, in: American Institute of Chemical Engineers (AIChE), New Orleans, 2014: p. 10. https://www.aiche.org/academy/videos/conference-presentations/unknown-aspects-metal-dust-explosions (accessed February 25, 2019).

[83] F. Lees, Lees' Loss Prevention in the Process Industries: Hazard Identification, Assessment and Control, Butterworth-Heinemann, Sam Mannan, 2012.

[84] R.A. Yetter, G.A. Risha, S.F. Son, Metal particle combustion and nanotechnology, Proc. Combust. Inst. 32 (2009) 1819–1838. doi:10.1016/j.proci.2008.08.013.

[85] G. Risha, Y. Huang, R. Yetter, V. Yang, Experimental Investigation of Aluminum Particle Dust Cloud Combustion, in: 43rd AIAA Aerosp. Sci. Meet. Exhib., American Institute of Aeronautics and Astronautics, 2005. doi:10.2514/6.2005-739.

[86] C. Parr, T. Johnson, Evaluation of advanced fuels for underwater propulsion, in: 2003.

[87] Y. Huang, G.A. Risha, V. Yang, R.A. Yetter, Effect of particle size on combustion of aluminum particle dust in air, Combust. Flame. 156 (2009) 5–13.

[88] Y. Huang, G.A. Risha, V. Yang, R.A. Yetter, Combustion of bimodal nano/micron-sized aluminum particle dust in air, Proc. Combust. Inst. 31 (2007) 2001–2009. doi:10.1016/j.proci.2006.08.103.

[89] H. Schneider, C. Proust, Determination of turbulent burning velocities of dust air mixtures with the open tube method, J. Loss Prev. Process Ind. 20 (2007) 470–476. doi:10.1016/j.jlp.2007.04.035.

[90] R. Lomba, P. Laboureur, C. Dumand, C. Chauveau, F. Halter, Determination of aluminum-air burning velocities using PIV and Laser sheet tomography, Proc. Combust. Inst. 37 (2019) 3143–3150. doi:10.1016/j.proci.2018.07.013.

[91] M. McRae, P. Julien, S. Salvo, S. Goroshin, D.L. Frost, J.M. Bergthorson, Stabilized, flat iron flames on a hot counterflow burner, Proc. Combust. Inst. 37 (2019) 3185–3191. doi:10.1016/j.proci.2018.06.134.

[92] H. Jiang, M. Bi, B. Li, D. Ma, W. Gao, Flame inhibition of aluminum dust explosion by NaHCO3 and NH4H2PO4, Combust. Flame. 200 (2019) 97–114. doi:10.1016/j.combustflame.2018.11.016.

[93] P. Julien, J. Vickery, S. Goroshin, D.L. Frost, J.M. Bergthorson, Freely-propagating flames in aluminum dust clouds, Combust. Flame. 162 (2015) 4241–4253. doi:10.1016/j.combustflame.2015.07.046.

[94] J. Sun, R. Dobashi, T. Hirano, Concentration profile of particles across a flame propagating through an iron particle cloud, Combust. Flame. 134 (2003) 381–387. doi:10.1016/S0010-2180(03)00137-8.

[95] M. Silvestrini, B. Genova, F.J. Leon Trujillo, Correlations for flame speed and explosion overpressure of dust clouds inside industrial enclosures, J. Loss Prev. Process

Ind. 21 (2008) 374–392. doi:10.1016/j.jlp.2008.01.004.

[96] V. Tonetto, Esplosioni di polveri organiche naturali: sviluppo di una formula empirica per la protezione di volumi confinati con superfici di sfogo , PhD thesis (In Italian), Università Degli Studi Della Tuscia di Viterbo, 2009.